1

Structural and functional diversity of novel coronin-1C (CRN2) isoforms.

Charles-Peter Xavier[1,2], André Rosentreter[1], Jens Reimann[4], Susanne Cornfine[5], Stefan Linder[5], Vanessa van Vliet[5], Andreas Hofmann[6], Reginald O. Morgan[7], Maria-Pilar Fernandez[7], Maria Stumpf[1], Rolf Müller[1], Tajana Jungbauer[8], Rolf Schröder[8,9], Angelika A. Noegel[1,2,3], Christoph S. Clemen[1,2,*]

[1]Center for Biochemistry, Institute of Biochemistry I, Medical Faculty, [2]Center for Molecular Medicine, and [3]Cologne Excellence Cluster on Cellular Stress Responses in Aging-Associated Diseases (CECAD), University of Cologne, Germany
[4]Department of Neurology, University Hospital Bonn, Germany
[5]Institut für Prophylaxe und Epidemiologie der Kreislaufkrankheiten, Ludwig Maximilians-Universität, Germany
[6]Structural Chemistry, Eskitis Institute for Cell and Molecular Therapies, Griffith University, Australia
[7]Department of Biochemistry and Molecular Biology, University of Oviedo and University Institute of Biotechnology of Asturias, Oviedo, Spain
[8]Institute of Neuropathology, University Hospital Erlangen, Germany
[9]Department of Neurology, University Hospital Erlangen, Germany

Running title: coronin-1C (CRN2) isoforms

[*]Author for correspondence:
C. S. Clemen, Institute of Biochemistry I, Medical Faculty, University of Cologne, Joseph-Stelzmann-Strasse 52, 50931 Cologne, Germany
Phone: +49 221 478 6980, Fax: +49 221 478 6979,
E-Mail: christoph.clemen@uni-koeln.de

Summary

Coronin-1C (synonyms: coronin-3, CRN2), a WD40 repeat containing protein involved in cellular actin dynamics, is ubiquitously expressed in human tissues. Here we report on the identification and functional characterization of two novel coronin-1C isoforms, referred to as CRN2i2 and CRN2i3. These isoforms, which arise from an alternative first exon identified in intron 1 of the coronin-1C gene, associate with F-actin. Gel filtration assays suggest that the largest isoform 3 exists as a monomer, whereas the conventional isoform 1 and isoform 2 both form trimers. Structural modelling predicts that this difference of the oligomerization state results from an interaction of the elongated N-terminus of CRN2i3 with its C-terminal extension. Analyses of the coronin-1C gene disclosed a single promoter containing binding sites for myogenic regulatory factors. CRN2i3 is expressed in mature skeletal muscle tissue and in differentiated myogenic cell lines. In human skeletal muscle CRN2i3 is a structural component of postsynaptic neuromuscular junctions and thin filaments of myofibrils. In addition, CRN2i1 and i2 are enriched within the F-actin core structure of podosomes. Our findings postulate a role of CRN2 isoforms in the structural and functional organization of F-actin in highly ordered protein complexes.

Key words

CRN2, coronin-3, coronin-1C, coronin nomenclature, isoform, promoter, MyoD, skeletal muscle, sarcomeres, podosomes, oligomerization, motor end plate

Introduction

Phylogenetic analyses revealed twelve subfamilies of coronin proteins, comprising seven vertebrate paralogs and five subfamilies in nonvertebrate metazoa, fungi and protozoa, some of them unclassified so far [1]. Even though coronin protein involvement in actin-dependent processes appears primordial, the individual members of the coronin protein family contribute to largely different cellular functions (for an extensive review on coronin proteins see [2]). In general, coronins are widely expressed in cells and tissues and are involved in signal transduction, transcriptional regulation, remodelling of the cytoskeleton, and regulation of vesicular trafficking [3]. Coronin-1C is a short coronin protein [4] of 474 amino acids with a calculated molecular mass of 53 kDa in human and murine cells. The apparent molecular mass from SDS-PAGE analysis is approximately 57 kDa. At the subcellular level coronin-1C exists in two different pools, an actin cytoskeleton associated non-phosphorylated pool and a diffusely distributed phosphorylated cytosolic pool [5]. Coronin-1C has been identified as an actin filament-crosslinking and bundling protein [5; 6] involved in distinct cellular functions like proliferation, migration, formation of cellular protrusions, endocytosis and secretion [7]. In addition, functional studies in human diffuse gliomas revealed an association of coronin-1C with tumor cell proliferation, motility and invasion, together contributing to the malignant phenotype of human diffuse gliomas [8]. Coronin-1C has also been found to be aberrantly regulated in other types of clinically aggressive cancers such as malignant melanoma [9].

Two nomenclature systems are currently used for coronin proteins. Both do not cover all coronin subfamilies and, moreover, do not allow unambiguous labelling of gene duplications and isoforms. These disadvantages initiated a comprehensive revision of the coronin protein nomenclature [1]. Based on evolutionary history, structural change and functional adaptation, the twelve coronin subfamilies were united and re-

numerated. 'CRN2' has been proposed as the new symbol for coronin-1C (current official symbol: CORO1C) or coronin-3 (most common synonym) [1]. Gene duplications in some vertebrates, for example in *Xenopus laevis*, resulted in two different coronin-1C proteins. Accordingly, they were named CRN2a and CRN2b [10]. In this study, we report on the functional and structural diversity of three human coronin-1C isoforms, designated as CRN2i1, CRN2i2 and CRN2i3.

Results

Identification of three CRN2 proteins encoded by two mRNA species

CRN2 usually migrates as a diffuse band of approximately 57 kDa. Immunoblotting of HEK293 and undifferentiated C2F3 cell lysates with the CRN2 specific monoclonal antibody K6-444 [5] revealed that the diffuse band can be separated into two closely migrating bands of 57/58 kDa (later referred to as CRN2i1/CRN2i2 (coronin-1C isoform 1/isoform 2)) (Fig. 1A). Moreover, a second slower migrating protein of 60 kDa (later referred to as CRN2i3 (coronin-1C isoform 3)) can be detected in murine skeletal muscle and differentiating C2F3 myoblasts as well as in brain and heart tissue (Fig. 1A; figure 2B in reference [5]). This protein is the only CRN2 isoform present in mature murine, bovine and human skeletal muscle tissue.

Northern blot analysis from total RNA of different murine organs, ES-cells, and undifferentiated C2F3 myoblasts employing a full-length CRN2 cDNA as a probe resulted in a single band of about 4.0 kb. Highest expression levels were detected in murine ES-cells as well as in thymus, testis, kidney, heart, and brain tissue. Lung tissue and undifferentiated C2F3 myoblasts exhibited intermediate signal intensities. Lowest expression levels were detected in mature skeletal muscle and spleen tissue (data not shown). Consistently, during the differentiation process of C2F3 myoblasts the amount of CRN2 specific RNA levels decreased markedly (Fig. 1B).

The possibility of posttranslational modifications of the CRN2 protein that could lead to differences in the apparent molecular mass was investigated by means of high-resolution two-dimensional gel electrophoresis. A protein spot containing CRN2i3 from bovine skeletal muscle was identified by mass spectrometry, but its very low abundance resulted in only limited sequence coverage by peptide mass fingerprinting and rendered a further analysis of posttranslational modifications impossible. Instead, two-dimensional gel electrophoresis of protein samples from murine, bovine and

human skeletal muscle in conjunction with immunoblotting was performed. Putative

ubiquitinylation and sumoylation (SUMO1-3) of CRN2i3 could not be detected. In

contrast, phosphorylations were present in CRN2i3, but they did not contribute to the

observed difference in the molecular mass (data not shown).

Therefore, 5'-RACE, 5'-RLM-RACE, and RT-PCR protocols were employed and

resulted in the identification of additional transcripts. An alternative exon, exon 1b,

contains two more start codons that are in frame with the known start codon of CRN2

(Fig. 2) potentially elongating the 'conventional' CRN2 transcript (referred to as

isoform 1, CRN2v1, accession no. **NM_014325**) by addition of either 6 (referred to as

isoform 2, CRN2v2, accession no. **AM849477**) or 53 codons (referred to as

isoform 3, CRN2v3, accession no. **AM849478**). The longer isoform 3 encompasses

the sequence of the shorter isoform 2. On the genomic level, the novel exon 1b is

located within the previously proposed 30 kb intron 1 present between the 5'

untranslated exon, exon 1a, and the first coding exon, exon 2, of the 'conventional'

CRN2 sequence. Sequence derived predictions suggest three potential CRN2

protein isoforms (Tab. 1), with molecular masses of 53 kDa and a pI of 6.7 (CRN2i1,

NP_055140), 54 kDa and pI 6.9 (CRN2i2, **AM849477**), 59 kDa and pI 7.9 (CRN2i3,

AM849478), that correspond to the protein bands detected by mAb K6-444.

Evolutionary insight into CRN2 regulation

Three atypical ESTs initiating from within 3' intron 1 were detected for CRN2 from

human but not other species. Comparison of their common 5' segment, up to 282 bp

in gb:DC377708, with 39 orthologous mammalian promoters identified a putative

alternative exon 1b encoding the N-termini of CRN2i2 and CRN2i3 in five catarrhine

primates separated by less than 25 million years of evolution (viz. human,

chimpanzee, gorilla, orangutan and gibbon). All earlier diverging primates (i.e.

macaque, baboon, marmoset, tarsier, lemur and galago) and other mammals (eutherian, metatherian and prototherian) harboured either start codon mutations, frame shift deletions or splice site changes in their genomic sequences that precluded the generation of transcripts encoding CRN2i3. Only 3 of 11 primates (macaque, baboon and galago) and 6 of 19 other mammals (tree shrew, dog, horse, alpaca, rabbit and pika) retained the capacity to generate transcripts encoding the shorter CRN2i2.

High throughput techniques of physically isolating chromatin-bound pre-initiation complex proteins followed by DNA microarray sequencing and mapping to 5' transcript regions of the genome have previously identified a single active promoter in CRN2, despite evidence for alternative promoters in many other genes ([11], supplemental data). We mapped over 200 human 5' ESTs (Hs.706390) to this primary transcription start site (TSS) in CRN2 exon 1a with only minor variation among 40 other ESTs at sites ±9 bp (Fig. 2A). Data on 5' cDNA sequences derived from CAGE tag clusters for CRN2 provided reliable high throughput statistics to confirm the same unique TSS (http://gerg01.gsc.riken.jp/cage_analysis/). A prominent CpG island (G+C 64%) located from -900 to +1485 bp relative to this well-punctuated TSS supported this promoter characterization, while further upstream regions and intron 1a are replete with closely spaced repetitive elements such as Alu, MIR and Line1 that are more likely to disrupt gene regulation.

Sequence conservation of the core promoter among mammals established the functional importance of this region and highlighted several sequence motifs relevant to both general and specific transcriptional regulation. A profile hidden Markov model (pHMM) logo of the aligned sequences (Fig. 2B) illustrates the manner by which "phylogenetic footprinting" can localize evolutionary functional constraint through column height (i.e. probability of occurrence) and nucleotide frequencies. Myogenic

regulatory factors such as MyoD, Myf5, MRF4 and myogenin are known to control muscle-specific gene expression by forming hetero-dimers with E-proteins that bind E-box motifs (e.g. CACCTG) with candidate sites located in the CRN2 promoter region. Evolutionary analyses using the VISTA browser and rVISTA [12] identified other conserved, functionally relevant regulatory elements, including double representation of a prominent and strategically located motif UF1H3beta_Q6. This DNA element (TGCGGGGGAGGGGC or CGCGGGGGCGGGGC) contains internal subsites for NGFIC (EGF4), Klf4 and Sp1 (common to many core promoters defined by CpG islands) with conspicuous G-rich stretches. This may bear directly on MyoD regulation of CRN2 transcription as recent evidence identifies guanine-rich quadruplex structures of regulatory sequences as key binding elements for homo-dimeric MyoD [13].

The region between the upstream promoter and coding exon 2 was also subjected to comparative genomic analysis to investigate the origin of an alternative transcription start site near the 3' end on intron 1 (Fig. 2C). The genomic sequence capability was restricted to modern primates and the most 5' of three human ESTs came to within 36 bp of a well-conserved CAG motif, possibly reflecting the true end of intron 1a and a novel splice site demarcating alternative exon 1b of 291-317 bp in these primates. Evidence of exon-specific transcript expression can be visualized and quantified for individual cell types by exon chip microarray at the UCSC genome browser (http://genome.ucsc.edu/), but CRN2 alternative transcripts were not at a detectable level from these data. Finally, only 2 of the 1,100 single nucleotide polymorphisms catalogued for human CRN2 affect the coding sequence by aa change (Asp85Tyr) or frame-shift deletion (P203/Q204) and at present there are neither known splice site variations, regulatory SNPs nor disease associations among HapMap screened populations.

CRN2i3 is part of the myogenic differentiation program

While the ubiquitous CRN2i1/2 ("diffuse" band) appears to be expressed

constitutively, expression of the largest isoform CRN2i3 is specifically up-regulated

during myogenic differentiation. In contrast to undifferentiated C2F3 myoblasts,

differentiated C2F3 myotubes (eight days of differentiation) display mostly CRN2i3,

with only a trace of isoforms 1 and 2 (Fig. 1A). We monitored the switch from the

faster to the slower migrating isoforms by a time course experiment of differentiating

C2F3 cells. At day 0, before induction of differentiation, CRN2i1 and 2 were detected

in the C2F3 myoblasts. Low amounts of CRN2i3 were observed after three days of

differentiation, with a wide and diffusely migrating band corresponding to CRN2i1 and

2 below a thin band of CRN2i3 (Fig. 1C). Detection of annexin A7 was used as

control, since the large isoform of annexin A7 (51 kDa) is a marker of late (in vitro)

myogenesis and also appeared at day three [14]. CRN2i3 was exclusively found in

mature skeletal muscle (see below). To validate the specificity of CRN2i3 in the

myogenic differentiation program, we converted NIH3T3 fibroblasts, which only

express the CRN2i1 and 2, into myogenic cells by ectopic expression of MyoD [14].

Converted cells initiated expression of CRN2i3 (Fig. 1D). Similarly, MyoD expression

in C2F3 cells grown under non-differentiating conditions led to an expression of

CRN2i3.

Identical subcellular distribution, but different oligomerization state of the

CRN2 protein isoforms

Sucrose gradient fractionation of lysates of differentiated C2F3 myotubes

demonstrates a co-distribution of the three CRN2 isoforms (Fig. 3A). They were

present in fractions of low density (fractions 4-9) that contained part of the

membrane-associated cortical F-actin as well as Golgi membranes (β-COP staining).

A second pool of CRN2 was detected in fractions 15-18 that contain heavy

membranes like ER-membranes indicated by the presence of BiP/GRP78.

CRN2 (isoform 1) like other short coronin proteins forms homo-trimers.

Oligomerization is mediated by the C-terminal coiled coil domain [4; 15; 16]. Gel filtration

analysis of soluble fractions derived from murine kidney and skeletal muscle tissue

indicates that CRN2i1/2 of kidney is mainly present in fractions corresponding to a

molecular mass of 180 kDa, indicating the presence of at least a part of CRN2 in a

trimeric state. In contrast, CRN2i3 derived from skeletal muscle is present mostly in

fractions of approx. 60 kDa, corresponding to a monomer (Fig. 3B).

Structural models of CRN2 isoforms

The N-terminal domain of short coronin proteins consists of a seven-bladed β-

propeller, originally proposed by [17] and [7], known from other WD40 proteins, and

finally confirmed by the crystal structure of truncated CRN4 (synonyms: coronin-1A,

coronin-1) [18]. Using the structural information for CRN4, a refined alignment for

CRN2 has been produced, see figure 2 in [16]. Following the typical topology of WD40

repeat domain proteins, the first β-strand of a blade is provided by the last β-strand of

the preceding WD40-repeat [19; 20]. The N-terminal β-strand formed by residues 17-22

in CRN4 provides the first β-strand of the last propeller blade of the protein (Fig. 4A).

Therefore, we suggest that in CRN2i3, which harbors an N-terminal 53 amino acid

extension, residues 69-74 map onto this motif of CRN4, thus aligning residues 66-

402 of CRN2i3 with the seven-bladed β propeller fold (Fig. 4A).

Using PSIPRED [21], the additional amino acid sequence in CRN2i2 (aa 1-6) and

CRN2i3 (aa 1-53) is predicted to consist of one (isoform 2) or three (isoform 3) β-

strands (Fig. 4A). It is highly unlikely that the additional peptide will form an eighth

blade within the β-propeller. We rather suggest that the additional β-strands either form an independent domain or they interact with accessible secondary structure elements of the 'core' protein, for example by annealing to existing β-strands. Based on the three-dimensional structure of CRN2, in which the N- and C-termini of the coronin β propeller are in spatial vicinity (Fig. 4B; aa 7-400 of CRN2i1 are visualized), the additional secondary structure elements at the N-terminus may interact with a β-strand in the C-terminal extension or with residues of the coiled coil domain, and thus interfere with oligomerization.

GFP-fusion proteins of CRN2 isoforms localize to F-actin structures

The three isoforms of CRN2 were expressed as GFP-fusion proteins and their distribution was studied in HEK293 cells and in undifferentiated C2F3 myoblasts and differentiated C2F3 myotubes. Expression of the fusion proteins was confirmed by western blotting. Each fusion protein was visible as a single band and did not present tagged variants. C2F3 myotubes expressing CRN2i1 or CRN2i2 GFP-fusion proteins additionally displayed the endogenous CRN2i3 (data not shown). In general, all isoforms localized in a diffuse and punctuated manner in the cytosol (Fig. 5A-C, arrows), at the leading edges of lamellipodia and filopodia (double-arrows), at the submembranous area (arrowheads), and to F-actin fibers (double-arrowheads). In C2F3 myotubes the GFP-fusion proteins mainly localized to F-actin fibers. CRN2 was highly enriched in F-actin rich areas, with high signal intensities of CRN2 matching high signal intensities of F-actin. Significant differences of the CRN2 isoforms with regard to F-actin association or a general contribution to cellular function could not be observed as assessed by differential centrifugation and cell motility assays (data not shown).

CRN2 is a novel component of podosomes

Immunoblotting of podosome-enriched cell fractions from primary human macrophages indicated expression and potential podosomal localization of CRN2i1/2 (Fig. 6A). Immunofluorescence images using mAb K6-444 confirmed endogenous CRN2 as a novel component of podosomes (Fig. 6B). A comparable distribution of CRN2 proteins was seen in macrophages transfected with constructs encoding isoforms 1, 2, and 3 fused to GFP (Fig. 6C; only CRN2i1 is shown). Every podosome displayed an enrichment of CRN2 within the F-actin-rich core structure (arrows). In addition, CRN2 co-localized to submembranous F-actin structures of macrophages (Fig. 6D, arrowheads).

To address the question whether CRN2 is essential for the formation of podosomes a pool of CRN2-specific siRNAs was transfected into primary human macrophages. In contrast to cells transfected with a control (scrambled) siRNA, a significant reduction of the CRN2 protein started three days after transfection (Fig. 7A). Immunofluorescence images of macrophages still expressing (day 1 after transfection, Fig. 7B) and completely lacking endogenous CRN2 (day four after transfection, Fig. 7C) demonstrate normal podosomes. CRN2 knockdown did neither influence number, size, distribution, nor fluorescence intensity of podosomes.

CRN2i3 is a structural component of neuromuscular junctions and myofibrils

Based on our observation that mature skeletal muscle fibers exclusively express CRN2i3, transverse sections of human skeletal muscle were immunolabelled with mAb K6-444. In general, the antibody showed a relatively uniform distribution throughout the muscle fibres (data not shown). However, in a subset of muscle fibers subsarcolemmal enrichments of CRN2 were visible. Co-staining with FITC-labelled α-bungarotoxin demonstrated that these areas correspond to the postsynaptic area

and the junctional sarcoplasm of motor end-plates (Fig. 8, arrow). Longitudinal optic sections of single human muscle fibers labelled with CRN2 mAb revealed a striated CRN2 staining pattern. Co-stainings with an antibody against the M-band component myomesin (Fig. 9A) and an antibody against actin (Fig. 9B) showed that CRN2i3 is a component of the thin-filament of myofibrils.

Discussion

In the present study we identified two novel isoforms of CRN2 (synonyms: coronin-1C, coronin-3), named CRN2i2 and CRN2i3. They do not arise from post-translationally modified 'conventional' CRN2i1, but they are encoded by a common, alternatively spliced transcript. A novel alternative exon, exon 1b, which contains two more start codons, replaces an untranslated exon, now termed exon 1a, preceding the normal start codon present in exon 2 of the CRN2 gene. Accordingly, two transcripts differing at the 5' end code for three protein isoforms of CRN2 that vary in their N-terminal length. Expression of the largest CRN2 protein, CRN2i3, can be specifically induced by MyoD as part of the myogenic differentiation program, while the two smaller isoforms are repressed. CRN2i3 is the only CRN2 isoform present in mature skeletal muscle tissue and is expressed in low abundance.

The possibility that MyoD homo-dimers could bind directly to guanine-rich core promoter elements in CRN2 [13] might explain how it alters, directly or indirectly, the transcription start site specificity within the unique CRN2 promoter. The prospect that the novel protein isoforms 2 and 3 may originate from alternative processing of a single primary transcript requires validation by the eventual isolation of a composite, elongated transcript encoded by both exons 1a and 1b.

The mechanism by which myogenic regulatory factors operate on a single promoter to enhance transcript diversity by alternative processing of the primary transcript is known to involve RNA binding proteins such as MBNL and CELF, which have been genetically linked to several neuromuscular disorders [22]. The possibility should therefore be considered that such alternative splicing regulators play an accessory role downstream of MyoD to (de)stabilize or reconfigure a primary transcript comprising exons 1a, 1b and flanking introns (i.e. containing splicing factor binding

motifs) resulting in the excision of different segments and the formation of distinctly processed CRN2 transcripts during myogenic differentiation in primates.

The elongated N-terminus in CRN2i3 changed the oligomerization state of the protein. While CRN2 derived from kidney tissue (isoforms 1 and 2) forms trimers, CRN2i3 from skeletal muscle tissue eluted as a monomer from gel filtration experiments. Within the three-dimensional structure, the N- and C-terminal ends of the coronin β propeller are in spatial vicinity (Fig. 4A,B). From this, two scenarios for an interaction can be envisioned; (i) an interaction of the additional secondary structure elements in the elongated N-terminus of CRN2i3 with the β-strand formed by residues 438-442 in the C-terminal extension causes conformational changes and prevents the following helical domain from engaging in a coiled coil; (ii) amino acid residues 1-47 from the additional N-terminal peptide directly interact with residues 489-527 in the coiled coil domain and thus prevent formation of a coiled coil.

It remains to be seen how an interaction suggested in (ii) may be structurally achieved. Obviously, any direct interaction with a critical residue in 489-527 can potentially prevent formation of the coiled coil. Alternatively, despite no helix or coiled coil formation is predicted for residues 1-47, there are two intriguing motifs in the N-terminal domain of CRN2i3, namely NSWAKER (14-20) and APSIGER (37-43) (Fig. 4A). Both motifs conform to (*abcdefg*)$_n$, frequently found in coiled coils. As such, either one of the two motifs might interact with a region in the coiled coil domain, thereby preventing the formation of an inter-molecular coiled coil.

The current model depicting coronin function shows a dual regulation in the F-actin turnover [23]. 'Coronin' recruits the Arp2/3-complex to the barbed end and protects growing actin-filaments from depolymerisation, but promotes cofilin-dependent actin sequestration at the pointed end of actin filaments. Additionally, CRN2 [5; 6], CRN4 [24],

and further coronins [10] have been shown to bundle and crosslink F-actin in vitro. It is tempting to speculate that the oligomerization state of coronin proteins turns out as a mechanism controlling actin-related cellular functions. Intriguingly, both hepta-peptide motifs in the N-terminal domain of CRN2i3 contain predicted phosphorylation sites, where post-translational modifications might assist in regulation of the CRN2 activities.

Confocal analysis of endogenous CRN2 and of GFP-fusion proteins in various cells as well as differential centrifugation assays indicated a similar subcellular localization of the CRN2 isoforms. The GFP-fusion proteins associated with F-actin structures at cellular extensions and cytosolic F-actin fibers. In a previous study, we had reported that CRN2 is important for the induction of invadopodia in human glioblastoma cells (Thal et al., 2008). Related small dot-like dynamic structures at the cell-matrix border involved in cell invasion are podosomes. They also are enriched with F-actin and matrix degrading enzymes (Gimona et al., 2008; Linder, 2007) (www.invadosomes.org). Here, we used substrate-attached human primary macrophages that constitutively form well-defined podosomes [25] and could demonstrate that CRN2 is a novel component of the F-actin-rich core structure of podosomes. While CRN2 does not seem to be essential for the formation of podosomes, it may affect their lifetime, internal actin turnover or function such as in matrix degradation. The finding that CRN2 is essential for formation and function of invadopodia, but not for the formation of podosomes, points to a different regulation of these complex invasion-mediating structures.

Analyses of normal human skeletal muscle tissue showed a localization of CRN2i3 within the thin filament region of the sarcomere. Identification of novel components of the sarcomere is not uncommon. For example, myomesin-3 [26], CAP-2 [27] and

leiomodin [28] have been described recently. The physiological role of CRN2 within the thin filament structure is currently unclear. CRN2i3 may play a role either structurally, by organization of the sarcomere such as stabilization of the sarcomeric F-actin bundles, or functionally, e.g. in force development.

CRN2i3 further co-localized with the postsynaptic area and the junctional sarcoplasm of motor end-plates. Actin is also a known component of this structure [29], which is characterized by folds of the sarcolemma and clustered ligand-gated Na^+/K^+-channels [30; 31]. The actin cytoskeleton directly or indirectly seems to be involved in the formation and stabilization of the motor end-plate [29; 32; 33], however, the details are unknown. CRN2i3 presents as a novel candidate possibly involved in the formation of this part of the neuromuscular junction.

ADF/cofilin and related proteins have been identified as binding partners of coronin proteins [7; 23] together regulating the sequestration of actin monomers. In skeletal muscle cofilin-2 is thought to be involved in muscle function and regeneration [34]. Mutations of cofilin-2 lead to rare congenital nemaline myopathy (OMIM 601443) characterized by severe proximal muscle weakness and the presence of nemaline rod bodies [35]. The latter finding provides a possible pathophysiological link between cofilin-2 mutations and CRN2i3.

Our present study demonstrates the expression of three isoforms of CRN2. A single promoter comprising binding sites for myogenic regulatory factors and an alternative first exon are involved in their regulation. The isoforms differ in the N-terminal length and display an unequal oligomerization state and tissue specificity. The newly identified CRN2 isoforms localize at and possibly regulate F-actin rich structures such as podosomes and sarcomeres, and are therefore likely to play essential roles in cell adhesion/invasion and skeletal muscle function.

Materials and Methods

Western blotting and antibodies

For western blot analysis primary human macrophages, mammalian cell lines, tissue samples, and fractions of differential centrifugation and gel filtration experiments were mixed with SDS-sample buffer, sonicated, centrifuged, and samples of the supernatants were subjected to standard SDS-PAGE and western blotting [36; 37]. Two-dimensional gel electrophoresis in conjunction with immunoblotting was performed according to [38]. Incubation with primary antibody was followed by incubation with goat anti-mouse IgG coupled to horseradish peroxidase (Sigma); visualisation was done by enhanced chemiluminescence and exposure to X-ray films (Kodak). CRN2 was detected with mAb K6-444 [5]; mAb 203-217 specifically recognized annexin A7 [39]. ß-COP was detected using mAb maD [40], sarcomeric actin was recognized by mAb 5C5 (Sigma), and anti-BiP/GRP78 was from Transduction Laboratories. Furthermore a rabbit polyclonal antibody against myomesin (1:200; a gift from Peter van der Ven, Bonn), a rabbit polyconal antibody against desmin (1:200; 2203PDE; Euro-Diagnostica), a sheep polyclonal antibody against the skeletal muscle ryanodine receptor (RyR1; 1:100; 70372(27); Upstate Biotechnology; developed by Kevin P. Campbell), and a monoclonal antibody against actin (1:100; AC40; Sigma) were used.

Immunofluorescence and immunohistochemistry

Immunofluorescence imaging of cultured cell lines was performed according to [8]. All human skeletal muscle samples were taken from diagnostic biopsies that were found not to be abnormal by standard histological work-up. Isolation of human myofibers was performed by manual separation of fresh muscle biopsies in "relaxation solution" [41]. The fibres were then dried on glass slides and fixed in a 1:1 methanol acetone

mixture for 5 minutes at –20°C as were the 6 μm transversal cryo-sections of skeletal muscle. The sections used for double labelling with FITC-α-bungarotoxin (Sigma), however, were not fixed as this reduces the bungarotoxin signal intensity. For the detection of the primary antibodies Texas-Red-conjugated goat-anti-rabbit and donkey-anti-sheep secondary antibodies from Jackson Immunoresearch Lab (dilution 1:80), as well as isotype specific goat-anti-mouse antibodies from Molecular Probes conjugated with Alexa 555 or 488 (diluted 1:800 and 1:400, respectively) were employed. All staining and antibodies solutions were prepared in PBS, incubation with primary antibodies was overnight at 4°C, with secondary antibodies or FITC-alpha-bungarotoxin for one hour at room temperature. A Nikon H800 microscope equipped with a CCD-camera (Sony DXP-9100P 3CCD Color Video) and Lucia imaging software (LIM Laboratory Imaging Ltd), and a Leica TCS NT confocal microscope with Leica confocal software (version 2.00, build 0871) were used for analysis and documentation. Podosomes were visualized according to [25]. F-actin was stained with Alexa 568-labeled phalloidin (Molecular Probes).

Mammalian cell culture

HEK293 human embryonic kidney cells (ATCC: CRL-1573), C2F3 murine myoblasts ([14]; a subclone of C2C12 myoblasts, ATCC: CRL-1772), NIH3T3 murine fibroblasts (ATCC: CRL-1658), Bruce 4 ES-cells (C57BL/6J), and phoenix ecotropic packaging cells (ΦNX-E; gift of G. Nolan, Stanford University) were grown in standard nutrition media at 5% CO2 and 37°C. To induce differentiation of C2F3 myoblasts 0.2% horse serum replaced the fetal calf serum. Human peripheral blood monocytes were isolated and differentiated into macrophages as described previously [25].

For myogenic conversion of NIH3T3 fibroblasts a retrovirus derived from plasmid BMN-hMyoD-IRES-GFP (transfected into ΦNX-E cells) containing a cassette coding

for human MyoD was used [14]. Highly efficient transfection of primary human macrophages with a CRN2 specific siRNA-pool (Dharmacon siGENOME siRNA # M-017331-00) was performed according to [7] using a Microporator device (Peqlab). In vitro wound healing was performed as described earlier [7].

RNA purification, northern blotting, 5'-RACE, 5'-RLM-RACE, and RT-PCR

RNA-samples: Total RNA from cells was extracted using the RNeasy Mini kit (Qiagen); total RNA from murine tissues was prepared using a TRIzol (Invitrogen) protocol [42]; total RNA from samples of human skeletal muscle biopsies was prepared with RNA-Magic (Bio-Budget) following the manufacturer's protocol. In addition, a pool of RNA from adult human skeletal muscle was obtained from Clontech.

Northern blotting: 30 µg of total RNA from murine ES-cells, undifferentiated C2F3 myoblasts, differentiated C2F3 myotubes, various murine organs, and samples of human skeletal muscle tissue were analyzed by northern blotting using either a full-length murine CRN2 cDNA (accession no. **AF143957**) or a 160 bp PCR product specific for CRN2i3 (amplified by primer pair hCoro3cF/hCoro3cR, see below), and a ß-actin cDNA as probes.

5'-RACE: Standard 5'-RACE was performed on various samples of total RNA extracted from human skeletal muscle tissue. Reactions were carried out according to the manufacturer's protocol (Roche, 5'/3' RACE Kit 2nd Generation, #03353621001). Primers used were: SP1 primer (reverse, for cDNA synthesis) ACTAAGAAGCACATTGCGGGCCGT; Oligo d(T)-anchor primer (forward) GACCACGCGTATCGATGTCGACTTTTTTTTTTTTTTTT; SP2 primer (reverse, for 1st PCR with Oligo d(T)-anchor primer) CCATACCATGACCGTGCAGTCCTC; PCR anchor primer (forward) GACCACGCGTATCGATGTCGAC; SP3 primer (reverse, for

2nd nested PCR with PCR anchor primer) TCGACCAGTCTTGTGCAGAGGGAG.

The PCR products were cloned into pGEMTeasy vector (Promega) and sequenced.

5'-RLM-RACE: RLM (RNA-Ligase Mediated)-RACE allows the amplification of cDNA only from full-length capped mRNA and determines the real 5-prime end of an mRNA. 5'-RLM-RACE was performed on various samples of total RNA extracted from human skeletal muscle tissue and reactions were carried out according to the manufacturer's protocol (Ambion, FirstChoice RLM-RACE Kit, #1700). Reverse transcription using random decamers was carried out at 49°C. Primers used are 5'-RACE outer primer GCTGATGGCGATGAATGAACACTG, 5'-RACE inner primer CGCGGATCCGAACACTGCGTTTGCTGGCTTTGATG, in combination with various reverse primers for the first PCR (hCoro3R16 GATCGTTATGTGGGCACCAG, hCoro3R17o TCCAACGCGTGTGTGAAAGTGG, hCoro3R18o TGGCCTCTCTCCAATGCTGG) and second (nested) PCR (hCoro3R13 TGGTCATTTTTCACCGCTTGC, hCoro3R19i TGAAGTAAGAGACCCTTGGCAGG, hCoro3R20i TTGGCAGGCAATTGAGCATCC). PCR products were cloned into pGEMTeasy or purified and sequenced directly.

RT-PCRs: cDNA from human skeletal muscle total RNA was obtained using p(dN6)-oligomers and M-MLV reverse transcriptase (Promega) at 37°C for 1 h. PCRs were performed to confirm or expand the sequences of the different CRN2 clones identified by RACE. PCRs were carried out at 63°C annealing temperature; primers used were: hCoro3R13 TGGTCATTTTTCACCGCTTGC, hCoro3R16 GATCGTTATGTGGGCACCAG, hCoro3R17o TCCAACGCGTGTGTGAAAGTGG, hCoro3R18o TGGCCTCTCTCCAATGCTGG, hCoro3R19i TGAAGTAAGAGACCCTTGGCAGG, hCoro3R20i TTGGCAGGCAATTGAGCATCC, hCoro3F20c GGATGCTCAATTGCCTGCCAA, hCoro3F21c CTCAAAATGTATGGCCCTGGTAGTC, hCoro3F22c

TGGCCACGAATCATTTGCCATC, hCoro3F23c CAGCGGTTGGAGGCTTCG, hCoro3F24c CTTTGCAGCGGGGACTTCG. Fragments obtained were cloned into pGEMTeasy and sequenced or the PCR-products were purified and sequenced directly using a 377 ABI DNA-sequencer (Applied Biosystems).

Differential centrifugation, subcellular fractionation, and gel filtration

Differential centrifugation was done according to [5], isopycnic separation on a discontinuous sucrose gradient according to [14]. For gel filtration analysis 100 mg of murine skeletal muscle or kidney tissue were lysed in 20 mM HEPES, pH 7.2, 1 mM EDTA, protease inhibitor cocktail, and sonicated. The lysate was centrifuged for 30 min at 10,000 g, followed by centrifugation of the supernatant at 100,000 g for 1 h. The latter supernatant was adjusted to 0.6 M KCl, incubated for 1 h at 4°C, and re-centrifuged at 100,000 g for 1 h. KCl minimizes interactions between CRN2 and other proteins as well as interactions between actin and myosin [43]. The supernatants were adjusted to 1 µg/µl protein, and 50 µl were separated on a Superdex G200 gel filtration column using the SMART system (Amersham Biosciences).

Plasmids for expression of CRN2 isoforms

To express human EGFP-CRN2i1 ('conventional' coronin-1C isoform 1, accession no. **NM_014325**) in C2F3 myoblasts, an AgeI/BamHI EGFP-CRN2i1-837bp3'UTR cassette was retrieved from EGFP-CRN2i1 [5]), blunt ended and cloned into the BamHI/NotI backbone of pBMN-Z (Nolan, Stanford University). Retroviruses derived from the resulting plasmid EGFP-CRN2i1-BMN transfected into ΦNX-E cells were used to infect C2F3 target cells according to [14]. For expression of EGFP-CRN2i1 in HEK293 cells construct EGFP-CRN2i1 [5] was used; stably expressing cells were obtained after neomycin selection. Primary human macrophages were

transfected with EGFP-CRN2i1 using a microporator device (PeqLab; Erlangen, Germany) according to the manufacturer's instructions.

In vitro mutagenesis was employed to generate plasmids coding for the two additional isoforms. Plasmids EGFP-CRN2i1-BMN and EGFP-CRN2i1 were used as templates. Primer pair hCoro3bFmut (CGAGCTCAAGCTTCGAATTCTATGCGTTGGAAGGACACGATGAGGCGAGTGGTACG) and hCoro3bRevmut (CGTACCACTCGCCTCATCGTGTCCTTCCAACGCATAGAATTCGAAGCTTGAGCTCG) introduced or exchanged base pairs resulting in pEGFP- and pBMN-plasmids coding for CRN2i2 (coronin-1C isoform 2, accession no. **AM849477**).

Two steps were carried out to generate CRN2i3. First, primer pair hCoro3cF (GCCGAATTCGATGTATGGCCCTGGTAGTCAGC) and hCoro3cRev (CGCGAATTCGTGTGAAAGTGGCCTCTCTCCA) was used to amplify a CRN2i3-specific product with adjacent EcoRI restriction sites from a CRN2i3 5'-partial clone (see RACE/RT-PCR above) which was inserted into the EcoRI cut EGFP-CRN2i1-BMN and EGFP-CRN2i1 plasmids. Second, in vitro mutagenesis primer pair hCoro3cFmut (TGGAGAGAGGCCACTTTCACACATGCGTTGGAAGGACACGATGAGGCGAGTGGTACG) and hCoro3cRevmut (CGTACCACTCGCCTCATCGTGTCCTTCCAACGCATGTGTGAAAGTGGCCTCTCTCCA) introduced or exchanged base pairs resulting in pEGFP- and pBMN-plasmids coding for CRN2i3 (coronin-1C isoform 3, accession no. **AM849478**). All CRN2 expression constructs were verified by restriction enzyme digest and sequencing.

Bioinformatic analysis

Genomic sequence data for CRN2 from 11 primates and 28 other mammals were retrieved from NCBI (http://www.ncbi.nlm.nih.gov) and Ensembl (http://www.ensembl.org/Homo_sapiens/geneview?gene=ENSG00000110880). Regions encompassing the 5' promoter up to exon 2 were assembled, aligned by CLUSTALW and scrutinized bioinformatically for promoter features such as repetitive elements using REPEATMASKER (http://www.repeatmasker.org), CPGProD for CpG composition (http://pbil.univ-lyon1.fr/software/cpgprod.html), transcription start sites documented in dbTSS (http://dbtss.hgc.jp), coding regions and exon splice sites in RefSeq (NCBI) and regulatory elements in the TRANSFAC and JASPAR databases. Cap Analysis of Gene Expression (CAGE) tag clusters (http://gerg01.gsc.riken.jp/cage_analysis/), the cDNAs in dbTSS and the expressed sequence tag database (http://www.ncbi.nlm.nih.gov/dbEST/index.html) were searched to identify 5' transcripts and alternatively expressed exons by comparison with genomic sequences. Aligned promoter sequences were converted to an HMM model [44] and visualized as a sequence logo (http://www.sanger.ac.uk/Software/analysis/logomat-m/). Regulatory elements were mapped as species conserved regions by "phylogenetic footprinting" using FOOTPRINTER 3.0 (http://genome.cs.mcgill.ca/cgi-bin/FootPrinter3.0/FootPrinterInput2.pl), WEEDERH (http://159.149.109.9/modtools/) and rVISTA of the VISTA browser (http://genome-test.lbl.gov/vista/index.shtml), which identified potential DNA elements for transactivation factors.

Accession numbers

Nucleotide sequences of the two novel coronin-1C isoforms have been deposited at the European Molecular Biology Laboratory (EMBL) database. Accession numbers are **AM849477** (isoform 2, CRN2v2) and **AM849478** (isoform 3, CRN2v3).

Acknowledgements

References

1. Morgan, R. O. & Fernandez, M. P. (2008). Molecular Phylogeny and Evolution of the Coronin Gene Family. In *The Coronin Family of Proteins* (Clemen, C. S., Eichinger, L. & Rybakin, V., eds.), Vol. 48. Landes Bioscience & Springer. 978-0-387-09594-3, http://www.eurekah.com/chapter/3820

2. Clemen, C. S., Eichinger, L. & Rybakin, V. (2008). *The Coronin Family of Proteins*. Subcellular Biochemistry, 48, Landes Bioscience & Springer. 978-0-387-09594-3, http://www.eurekah.com/chapter/3785

3. de Hostos, E. L. (2008). A Brief History of the Coronin Family. In *The Coronin Family of Proteins* (Clemen, C. S., Eichinger, L. & Rybakin, V., eds.), Vol. 48. Landes Bioscience & Springer. 978-0-387-09594-3, http://www.eurekah.com/chapter/3790

4. Rybakin, V. & Clemen, C. S. (2005). Coronin proteins as multifunctional regulators of the cytoskeleton and membrane trafficking. *BioEssays* **27**, 625-632.

5. Spoerl, Z., Stumpf, M., Noegel, A. A. & Hasse, A. (2002). Oligomerization, F-actin interaction, and membrane association of the ubiquitous mammalian coronin 3 are mediated by its carboxyl terminus. *J. Biol. Chem.* **277**, 48858-48867.

6. Hasse, A., Rosentreter, A., Spoerl, Z., Stumpf, M., Noegel, A. A. & Clemen, C. S. (2005). Coronin 3 and its role in murine brain morphogenesis. *Eur. J. Neurosci.* **21**, 1155-1168.

7. Rosentreter, A., Hofmann, A., Xavier, C. P., Stumpf, M., Noegel, A. A. & Clemen, C. S. (2007). Coronin 3 involvement in F-actin-dependent processes at the cell cortex. *Exp. Cell Res.* **313**, 878-895.

8. Thal, D., Xavier, C. P., Rosentreter, A., Linder, S., Friedrichs, B., Waha, A., Pietsch, T., Stumpf, M., Noegel, A. & Clemen, C. (2008). Expression of coronin-3 (coronin-1C) in diffuse gliomas is related to malignancy. *J. Pathol.* **214**, 415-424.

9. Roadcap, D. W., Clemen, C. S. & Bear, J. E. (2008). The Role of Mammalian Coronins in Development and Disease. In *The Coronin Family of Proteins* (Clemen, C. S., Eichinger, L. & Rybakin, V., eds.), Vol. 48. Landes Bioscience & Springer. 978-0-387-09594-3, http://www.eurekah.com/chapter/3798

10. Xavier, C.-P., Eichinger, L., Fernandez, M. P., Morgan, R. O. & Clemen, C. S. (2008). Evolutionary and Functional Diversity of Coronin Proteins. In *The Coronin Family of Proteins* (Clemen, C. S., Eichinger, L. & Rybakin, V., eds.), Vol. 48. Landes Bioscience & Springer. 978-0-387-09594-3, http://www.eurekah.com/chapter/3808

11. Kim, T. H., Barrera, L. O., Zheng, M., Qu, C., Singer, M. A., Richmond, T. A., Wu, Y., Green, R. D. & Ren, B. (2005). A high-resolution map of active promoters in the human genome. *Nature* **436**, 876-880.

12. Loots, G. G., Ovcharenko, I., Pachter, L., Dubchak, I. & Rubin, E. M. (2002). rVista for comparative sequence-based discovery of functional transcription factor binding sites. *Genome Res.* **12**, 832-839.

13. Yafe, A., Shklover, J., Weisman-Shomer, P., Bengal, E. & Fry, M. (2008). Differential binding of quadruplex structures of muscle-specific genes regulatory sequences by MyoD, MRF4 and myogenin. *Nucleic Acids Res.* **36**, 3916-3925.

14. Clemen, C. S., Hofmann, A., Zamparelli, C. & Noegel, A. A. (1999). Expression and localisation of annexin VII (synexin) isoforms in differentiating myoblasts. *J. Muscle Res. Cell Motil.* **20**, 669-679.

15. Kammerer, R. A., Kostrewa, D., Progias, P., Honnappa, S., Avila, D., Lustig, A., Winkler, F. K., Pieters, J. & Steinmetz, M. O. (2005). A conserved trimerization motif controls the topology of short coiled coils. *PNAS* **102**, 13891-13896.

16. McArdle, B. & Hofmann, A. (2008). Coronin Structure and Implications. In *The Coronin Family of Proteins* (Clemen, C. S., Eichinger, L. & Rybakin, V., eds.), Vol. 48. Landes Bioscience & Springer. 978-0-387-09594-3, http://www.eurekah.com/chapter/3821

17. Gatfield, J., Albrecht, I., Zanolari, B., Steinmetz, M. O. & Pieters, J. (2005). Association of the leukocyte plasma membrane with the actin cytoskeleton through coiled coil-mediated trimeric coronin 1 molecules. *Mol. Biol. Cell* **16**, 2786-2798.

18. Appleton, B. A., Wu, P. & Wiesmann, C. (2006). The crystal structure of murine coronin-1: A regulator of actin cytoskeletal dynamics in lymphocytes. *Structure* **14**, 87-96.

19. Hudson, A. M. & Cooley, L. (2008). Phylogenetic, Structural and Functional Relationships between WD- and Kelch-Repeat Proteins. In *The Coronin Family of Proteins* (Clemen, C. S., Eichinger, L. & Rybakin, V., eds.), Vol. 48. Landes Bioscience & Springer. 978-0-387-09594-3, http://www.eurekah.com/chapter/3791

20. Smith, T. F. (2008). Diversity of WD-Repeat Proteins. In *The Coronin Family of Proteins* (Clemen, C. S., Eichinger, L. & Rybakin, V., eds.), Vol. 48. Landes Bioscience & Springer. 978-0-387-09594-3, http://www.eurekah.com/chapter/3787

21. McGuffin, L. J., Bryson, K. & Jones, D. T. (2000). The PSIPRED protein structure prediction server. *Bioinformatics* **16**, 404-405.

22. Yuan, Y., Compton, S. A., Sobczak, K., Stenberg, M. G., Thornton, C. A., Griffith, J. D. & Swanson, M. S. (2007). Muscleblind-like 1 interacts with RNA hairpins in splicing target and pathogenic RNAs. *Nucleic Acids Res.* **35**, 5474-5486.

23. Gandhi, M. & Goode, B. L. (2008). Coronin: The Double-Edged Sword of Actin Dynamics. In *The Coronin Family of Proteins* (Clemen, C. S., Eichinger, L. & Rybakin, V., eds.), Vol. 48. Landes Bioscience & Springer. 978-0-387-09594-3, http://www.eurekah.com/chapter/3812

24. Galkin, V. E., Orlova, A., Brieher, W., Kueh, H. Y., Mitchison, T. J. & Egelman, E. H. (2008). Coronin-1A stabilizes F-actin by bridging adjacent actin protomers and stapling opposite strands of the actin filament. *J. Mol. Biol.* **376**, 607-613.

25. Linder, S., Nelson, D., Weiss, M. & Aepfelbacher, M. (1999). Wiskott-Aldrich syndrome protein regulates podosomes in primary human macrophages. *Proc Natl Acad Sci U S A* **96**, 9648-9653.

26. Schoenauer, R., Lange, S., Hirschy, A., Ehler, E., Perriard, J. C. & Agarkova, I. (2008). Myomesin 3, a novel structural component of the M-band in striated muscle. *J. Mol. Biol.* **376**, 338-351.

27. Peche, V., Shekar, S., Leichter, M., Korte, H., Schroder, R., Schleicher, M., Holak, T. A., Clemen, C. S., Ramanath, Y. B., Pfitzer, G., Karakesisoglou, I. & Noegel, A. A. (2007). CAP2, cyclase-associated protein 2, is a dual compartment protein. *Cell. Mol. Life Sci.* **64**, 2702-2715.

28. Chereau, D., Boczkowska, M., Skwarek-Maruszewska, A., Fujiwara, I., Hayes, D. B., Rebowski, G., Lappalainen, P., Pollard, T. D. & Dominguez, R. (2008). Leiomodin is an actin filament nucleator in muscle cells. *Science* **320**, 239-243.

29.   Hall, Z. W., Lubit, B. W. & Schwartz, J. H. (1981). Cytoplasmic actin in postsynaptic structures at the neuromuscular junction. *J. Cell Biol.* **90**, 789-792.

30.   Ogata, T. (1988). Structure of motor endplates in the different fiber types of vertebrate skeletal muscles. *Arch. Histol. Cytol.* **51**, 385-424.

31.   Guth, L. (1983). An overview of motor unit structure and function. *Arch. Phys. Med. Rehabil.* **64**, 408-411.

32.   Berthier, C. & Blaineau, S. (1997). Supramolecular organization of the subsarcolemmal cytoskeleton of adult skeletal muscle fibers. A review. *Biol. Cell* **89**, 413-434.

33.   Dobbins, G. C., Zhang, B., Xiong, W. C. & Mei, L. (2006). The role of the cytoskeleton in neuromuscular junction formation. *J. Mol. Neurosci.* **30**, 115-118.

34.   Thirion, C., Stucka, R., Mendel, B., Gruhler, A., Jaksch, M., Nowak, K. J., Binz, N., Laing, N. G. & Lochmuller, H. (2001). Characterization of human muscle type cofilin (CFL2) in normal and regenerating muscle. *Eur. J. Biochem.* **268**, 3473-3482.

35.   Emery, A. E. H. (1999). *Neuromuscluar disorders: Clinical and Molecular Genetics*, Wiley, New York. 0-471-97817-5,

36.   Towbin, H., Staehelin, T. & Gordon, J. (1979). Electrophoretic transfer of proteins from polyacrylamide gels to nitrocellulose sheets: procedure and some applications. *Proc Natl Acad Sci U S A* **76**, 4350-4354.

37.   Laemmli, U. K. (1970). Cleavage of structural proteins during the assembly of the head of bacteriophage T4. *Nature* **227**, 680-685.

38.   Clemen, C. S., Fischer, D., Roth, U., Simon, S., Vicart, P., Kato, K., Kaminska, A. M., Vorgerd, M., Goldfarb, L. G., Eymard, B., Romero, N. B., Goudeau, B., Eggermann, T., Zerres, K., Noegel, A. A. & Schroder, R. (2005). Hsp27-2D-gel electrophoresis is a diagnostic tool to differentiate primary desminopathies from myofibrillar myopathies. *FEBS Lett.* **579**, 3777-3782.

39.   Selbert, S., Fischer, P., Pongratz, D., Stewart, M. & Noegel, A. A. (1995). Expression and localization of annexin VII (synexin) in muscle cells. *J. Cell Sci.* **108 (Pt 1)**, 85-95.

40.   Pepperkok, R., Scheel, J., Horstmann, H., Hauri, H. P., Griffiths, G. & Kreis, T. E. (1993). Beta-COP is essential for biosynthetic membrane transport from the endoplasmic reticulum to the Golgi complex in vivo. *Cell* **74**, 71-82.

41.   Vielhaber, S., Kunz, D., Winkler, K., Wiedemann, F. R., Kirches, E., Feistner, H., Heinze, H. J., Elger, C. E., Schubert, W. & Kunz, W. S. (2000). Mitochondrial DNA abnormalities in skeletal muscle of patients with sporadic amyotrophic lateral sclerosis. *Brain* **123 (Pt 7)**, 1339-1348.

42.   Chomczynski, P. & Sacchi, N. (1987). Single-step method of RNA isolation by acid guanidinium thiocyanate-phenol-chloroform extraction. *Anal. Biochem.* **162**, 156-159.

43.   Berryman, M., Gary, R. & Bretscher, A. (1995). Ezrin oligomers are major cytoskeletal components of placental microvilli: a proposal for their involvement in cortical morphogenesis. *J. Cell Biol.* **131**, 1231-1242.

44.   Eddy, S. R. (1998). Profile hidden Markov models. *Bioinformatics* **14**, 755-763.

45.   Bryson, K., McGuffin, L. J., Marsden, R. L., Ward, J. J., Sodhi, J. S. & Jones, D. T. (2005). Protein structure prediction servers at University College London. *Nucl. Acids Res.* **33**, W36-W38.

46.   Gringel, A., Walz, D., Rosenberger, G., Minden, A., Kutsche, K., Kopp, P. & Linder, S. (2006). PAK4 and alphaPIX determine podosome size and number

in macrophages through localized actin regulation. *J. Cell. Physiol.* **209**, 568-579.

Table legends

Table 1

Isoforms of CRN2 due to different N-terminal extensions. Amino acid sequence derived predictions suggest three different proteins with molecular masses (kDa) and pI values of 53/6.7, 54/6.9, and 59/7.9, respectively. New symbols for protein (and mRNA), CRN2i1 (CRN2v1), CRN2i2 (CRN2v2) and CRN2i3 (CRN2v3), according to [1].

Figure legends

Figure 1

A slower migrating isoform of CRN2 appears during myogenesis. **A**, lysates of HEK293 cells, murine skeletal muscle tissue, C2F3 myoblasts, and C2F3 myotubes (diff.) were analyzed by SDS-PAGE followed by western blotting using mAb K6-444 specific for CRN2 [5]. **B**, 20 µg of total RNA from C2F3 myoblasts and 50 µg of total RNA from myotubes (diff.) were subjected to gel electrophoresis under denaturing conditions and analyzed by northern blotting using a full-length CRN2 cDNA as probe; for control, the ethidium bromide stained RNA-gel is shown. **C**, time course of differentiation of C2F3 myoblasts. Cells were harvested at the indicated time points (day after initiation of differentiation) and analyzed by immunoblotting using mAb K6-444 and mAb 203-217 specific for annexin A7 as a control of myogenic differentiation. **D**, myogenic conversion of NIH3T3 fibroblasts using a retroviral vector encoding human MyoD. CRN2 from hMyoD-transduced and untransduced NIH3T3 and hMyoD-transduced, differentiated and undifferentiated C2F3 myoblasts is shown. Cells were harvested four days after transduction or after five days of differentiation, and analyzed by SDS-PAGE followed by western blotting using the CRN2 and annexin A7 specific antibodies.

Figure 2

Promoter and splicing architecture of 5' CRN2. **A**, the current reference assembly for CRN2 (NC_000012.10) was characterized for repetitive elements, CpG composition, transcription start site(s) in dbTSS and known exon splice sites. **B**, promoter sequences from -300 to +100 bp for CRN2 were aligned, converted to an HMM model and visualized as a sequence logo representing 12 mammalian species (i.e. human, orangutan, marmoset, macaque, cow, pig, vampire bat, guinea pig, mouse, rat, dog and opossum). The transcription start site (TSS) was designated by genomic mapping of external database CAGE, EST and full-length cDNA tags. Conserved motifs in the core promoter were characterized by phylogenetic footprinting programs, which identified the doubly represented element UF1H3beta_Q6. **C**, the alternatively spliced region is shown as a genomic DNA sequence logo derived from 11 primates capable of generating transcripts for both isoforms 2 and 3 (human, chimp, orangutan, gibbon), isoform 2 only (macaque, baboon, galago, tree shrew) or neither (marmoset, lemur, tarsier). Three human ESTs encoded by exon 1b giving rise to protein isoforms 2 and 3 are preceded by a putative, alternative intron 1a splice site.

Figure 3

Subcellular localization of CRN2 isoforms. **A**, fractionation of cell lysates from differentiated C2F3 myotubes by sucrose gradient centrifugation. Fractions were collected and analyzed by SDS-PAGE followed by western blotting using the antibodies K6-444 (CRN2), mAb AC 40 (ß-actin; Sigma), anti-BiP/GRP 78 (Transduction Laboratories), and maD (ß-COP; [40]). Arrow heads indicate the position of the slower migrating isoform 3. **B**, gel filtration analysis of cytoskeletal protein

extracts (100,000 g supernatant) of murine kidney and skeletal muscle tissue using a Superdex G200 column. Fractions were collected and analyzed by SDS-PAGE followed by western blotting using mAb K6-444, mAb AC 40, and mAb 5C5 (sarcomeric-actin; Sigma). The molecular mass is given.

Figure 4

A, Structure-based sequence alignment of CRN2 with CRN4. The CRN4 (synonyms: coronin-1A, coronin-1) amino acid sequence is sectioned according to the fold observed in the crystal structure [18]. The amino acid sequence of all three isoforms of CRN2 is aligned to CRN4 using amino acid sequence similarity as well as predicted secondary structure elements. The secondary structure of CRN2 was predicted using PsiPred [45] and is annotated in the lines shown as 'pred' (H: helix, E: strand, C: coil). The first amino acids of CRN2i1, CRN2i2 and CRN2i3 are indicated. The motifs printed in bold are similar to the heptad repeat motifs found in coiled coils. Potential phosphorylation sites in the N-terminal region of CRN2 are underlined. **B,** Homology model of CRN2 β propeller and C-terminal extension domains. The homology model of CRN2 (isoform 1; aa 7-400) was generated as reported earlier [7]. The N-terminal region is colored blue, the WD40 repeat domain (β propeller domain) is shown in aqua, and the C-terminal extension domain is shown in brown. Additional amino acids of isoforms 2 and 3 are fused to the N-terminal region and, in the case of isoform 3, can possibly extend to interact with the C-terminal extension domain and/or the coiled coil domain.

Figure 5

Subcellular localization of CRN2 isoforms expressed as GFP-fusion proteins. **A,** undifferentiated C2F3 myoblasts expressing EGFP-CRN2i1; **B,** differentiated C2F3

myotubes expressing EGFP-CRN2i3; **C**, HEK293 cells expressing EGFP-CRN2i2. Cells were fixed with formaldehyde. Green, fluorescence signal of EGFP-fused CRN2 isoforms, red, F-actin staining with TRITC-phalloidin. Arrowhead, submembranous localization; double-arrow, lamellipodial and filopodial enrichments of CRN2; arrow, dot-like structures at the bottom of the cell; double-arrowhead, localization of CRN2 to actin fibers.

Figure 6

CRN2 is a component of podosomes. **A**, fractions of human primary macrophages enriched in podosomes, bovine skeletal muscle tissue, control fractions devoid of podosomes [46], C2F3 myotubes, macrophages, and 10T1/2 fibroblasts were analyzed by SDS-PAGE followed by western blotting using mAb K6-444 specific for CRN2. **B**, confocal images demonstrate an enrichment of endogenous CRN2 at podosomes of primary human macrophages, fixed with formaldehyde and stained with mAb K6-444. **C**, primary human macrophages transfected with EGFP-fused CRN2i1. **D**, enlarged view of a GFP-CRN2i1 positive human primary macrophage. Arrow, localization of CRN2 in podosomes; arrowhead, submembranous enrichment of CRN2.

Figure 7

CRN2 knockdown does not affect podosome formation. **A**, effective siRNA-mediated knockdown of CRN2 in human macrophages. Western blotting confirms a strong reduction in the expression level three days after transfection, and no CRN2 is detectable at four days. β-actin staining used as control. **B,C**, confocal images of double-labelled human macrophages. **B**, cells one day after transfection expressing CRN2 and **C**, cells four days after transfection lacking CRN2 both show normal patterns of podosomes.

Figure 8

CRN2i3 co-localizes with the motor end plate. Immunostaining for endogenous CRN2 in transversal cryosections of mature human skeletal muscle frequently indicates subsarcolemmal enrichments. Double stainings with FITC-labelled α-bungarotoxin indicate a co-localization of CRN2 at postsynaptic area and the junctional sarcoplasm of the motor end plate (arrow). Note that the intensity of CRN2-staining as well as background levels in both channels differ from normal staining procedures by the lack of fixation to preserve α-bungarotoxin reactivity.

Figure 9

CRN2i3 targets to thin filaments of myofibrils. Human myofibers were isolated, double-labelled, and images were taken by confocal microscopy. **A**, co-staining with myomesin indicates a gap (arrows) between CRN2 and the M-band. **B**, co-staining with actin demonstrates a specific co-localization of CRN2 with sarcomeric actin.

Table 1

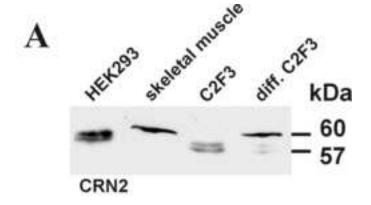Isoforms of CRN2 due to different N-terminal extensions

```
MYGPGSQLGKSGNNSWAKERGCSIACQGSLTSARLHAPSIGERPLSHMRWKDTMRRVVRQSKFRHVFG
QAVKNDQCYDDIRVSRVTWDSSFCAVNPRFVAIIIEASGGGAFLVLPLHKTGRIDKSYPTVCGHTGPV
LDIDWCPHNDQVIASGSEDCTVMVWQIPENGLTLSLTEPVVILEGHSKRVGIVAWHPTARNVLLSAGC
DNAIIIWNVGTGEALINLDDMHSDMIYNVSWNRNGSLICTASKDKKVRVIDPRKQEIVAEKEKAHEGA
RPMRAIFLADGNVFTTGFSRMSERQLALWNPKNMQEPIALHEMDTSNGVLLPFYDPDTSIIYLCGKGD
SSIRYFEITDESPYVHYLNTFSSKEPQRGMGYMPKRGLDVNKCEIARFFKLHERKCEPIIMTVPRKSD
LFQDDLYPDTAGPEAALEAEEWFEGKNADPILISLKHGYIPGKNRDLKVVKKNILDSKPTANKKCDLI
SIPKKTTDTASVQNEAKLDEILKEIKSIKDTICNQDERISKLEQQMAKIAA–
```
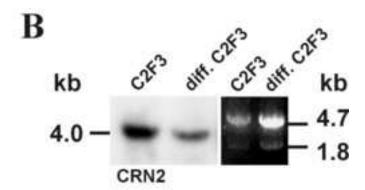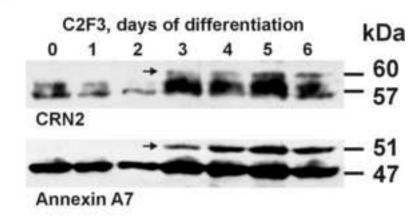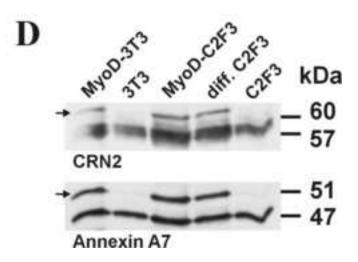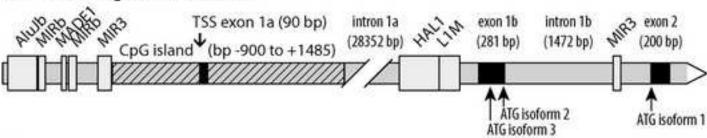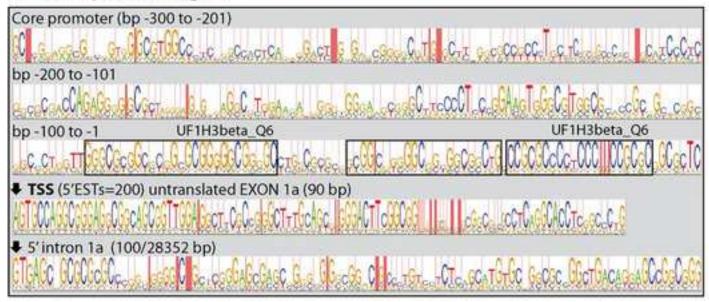
CRN2i3   **CRN2i2**   **CRN2i1**

Figure 2
Click here to download high resolution image

A CRN2 5′genomic features

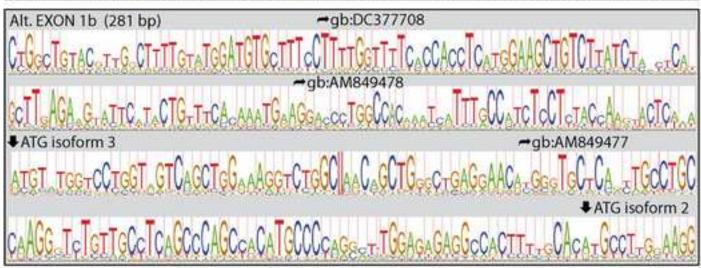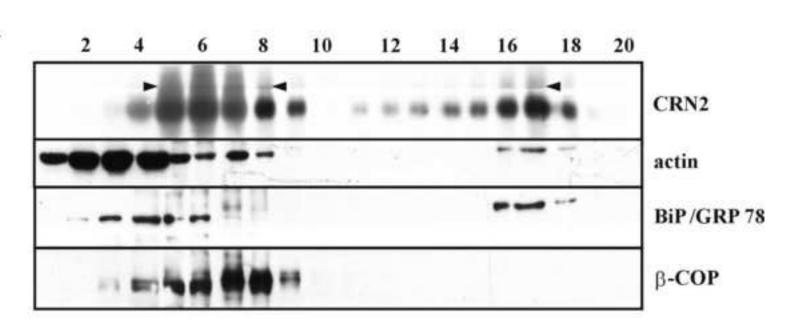B CRN2 promoter region

C CRN2 alternatively spliced region

Figure 4
[Click here to download high resolution image]
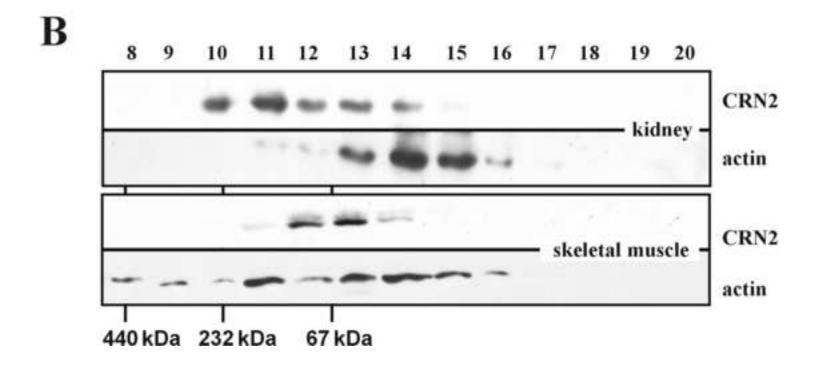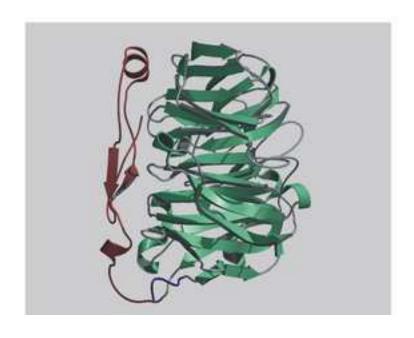
A

N-TERMINUS

| CRN213 |

```
                 |CRN213                                        |CRN212|CRN211
CRN4                                                  MGR QVVRSSK FRN        13
CRN213   MVGPGSQLGRSGRNSWAKER GCSI ACQGS LTSA RLHAPSIGERF LGHMRN HITHR RVVRQSK FBH   65
pred     CCCCCCCCCCCCCCCCCCCCC EEEE CCCCC EEEE CCCCCCCCCCC EEEEEE CCCCC EEEEEEE CCC
```

7-BLADED BETA-PROPELLER

```
STRAND            |--1--|              |-2--|      |-3--|        |+4--|
CRN4                                              VFG        QPAKAD QCYEDVRVS     31
CRN213                                            VFG        QAVEND QCYDDIRVS     83
pred                                              CCC        CCCCCC CCCCCEEEE

CRN4     QTTWD  SGFCAVN FK          FMALIC EASGGS AFLVLP LGHTGRVD KNV  FLVC      78
CRN213   RVTWD  SSFCAVN FR          FVAIII EASGGS AFLVLP LHGTGRID KSY  PTVC      130
pred     ECCCC  CEEEEKKC CC         CCCKEE EECCCC EEEEEE CCCCCCCC CCE  EEEE

CRN4     GHTAF  VLDIANC FHHDH       VIAGGS EDC    TVMVHE IPDGGLVLPL REPV  VTLE   128
CRN213   GHTGF  VLDIDWC FHNDQ       VIASGS EDC    TWGVHQ IPENGLTLSL TEPV  VILE   180
pred     ECCCC  EEEEEEC CCCCC       EEEEEC CCC    EEEEEE ECCCCCCCC CCEE  EEEE

CRN4     GHTNR  VGIVANH FTAQN       VLLSAG CDN    VILVWG VGTG    AAV  LTLSPD     173
CRN213   GHSNR  VGIVANH FTARN       VLLSAG CDN    AIIIWN VGTG    EAL  INLDD-     224
pred     CCCCC  EEEEEEC CCCCC       EEEEEE CCC    EEEEEE CCCC    CEE  EEEEC

CRN4     VHFDT  IYSVINS RDSA        LICTPC RDK    RVRVIE PRNG    TVV  AEKDR      216
CRN213   MHHDIM IYNVSNN RNGS        LICTAS RIK    RVRVID PRNQ    EIV  AEKEK      267
pred     CCCCC  EEEEEEC CCCC        EEEEKC CCC    EEEEEE CCCC    CEE  EEECC

CRN4     PHEGTR FVHAVFV SSG         KILTTG FSRMSER QVALWD THHLE  EFL  SLQSLD     265
CRN213   ANEGAK FMRAIFL ADG         NVFTTG FNROSER QLALNN FNGMQ  EFI  ALHRMD     316
pred     CCCCCC EEEEEEE CCC         CEEEEC CCCCCCC EEEEEE CCCCC  CEE  EEESCC

CRN4     TSSG   VLLFFFD FDTH        IVYLCG FGIS   SIRYFE ITSEAPF LHYL  SHF       310
CRN213   TSNG   VLLFFYD FUTS        IIYLCG FGIS   SIRYFE ITDESPY VHYL  NT-       360
pred     CCCC   EEEEEEC CCCC        EEEEEE CCCC   EEEEEE CCCCCEE EEEE  CU

CRN4     SSKES  QRGMGVM PKRGLEVNKCEIA RFYKLH ER   KCEFIA MT                      351
CRN213   FSSGEP QRGMGVM PKRGLGVNKCEIA RFFKLH ER   KCEFII MT                      402
pred     CCCCCC EEEEEEC CCCCCERECCCCC CEEEEE CC   CCCKEE EE
```

C-TERMINAL EXTENSION

```
CRN4    VFRES DLFQEIL YPPTAGPDPALT AEEWL GGRDAS PLLIS LNDGYVPPHSREL RVN R--GLDS---ARRAATPEFSGTPSSOT--V   430
CRN213  VFRES DLFQDDL VFCTAGPEAALE AEENF EGRNAD FILIS LKDNYIFGHNRDL KVV KVNILDSKPTANRKCDLISIPHGYTDTASV   480
pred    ECCCC EEEEEEE CCCCCCCCCCCC HHHHH CCCCC EEEEE CCCCCCCCCCCCC EEE CCCCCCCCCCCCCCCCCCCCCCCCCCCCCC
```

COILED-COIL

```
CRN4    SRLEED VRHLNAI ------- VQHLQEA LSRLEET VQAK---                           461
CRN213  QHEAKL DEILKEI KSIKDT ICNQDER ISDLEQQ -MAKIAA                            527
pred    CCCHHH HHHHHHH HHHHHH HHGCCHH HHGHHHH HHHHCC
```

B

Figure 5
Click here to download high resolution image

A

CRN2

B

CRN2

CRN2i1

phalloidin

merge

C

D

A

kDa

57 —

CRN2

43 —

actin

B

CRN2   phalloidin   merge

CRN2 siRNA -1d

C

10 μm

CRN2 siRNA -4d

Figure 9
Click here to download high resolution image